PHYSICAL REVIEW D VOLUME 28, NUMBER 2 15 JULY 1983

Phase structure, magnetic monopoles, and vortices in the lattice Abelian Higgs model

J. Ranft, J. Kripfganz, and G. Ranft
Sektion Physik, Karl-Marx-Universität, Leipzig, German Democractic Republic
(Received 20 July 1982)

We present Monte Carlo calculations of lattice Abelian Higgs models in four dimensions and with charges of the Higgs particles equal to $q=1$, 2, and 6. The phase transitions are studied in the plane of the two coupling constants considering separately average plaquette and average link expectation values. The density of topological excitations is studied. In the confinement phase we find finite densities of magnetic-monopole currents, electric currents, and vortex currents. The magnetic-monopole currents vanish exponentially in the Coulomb phase. The density of electric currents and vortex currents is finite in the Coulomb phase and vanishes exponentially in the Higgs phase.

I. INTRODUCTION

Following the work of Wilson[1] and Creutz,[2] the Monte Carlo calculation of lattice gauge theories has emerged as a valuable tool to study the phase structure of Abelian and non-Abelian gauge theories in the region of strong and intermediate couplings.

The analogy of electric confinement of charges in the strong-coupling region of Abelian and non-Abelian gauge theories with the Meissner effect in superconductors has been discussed repeatedly during the last few years. Monte Carlo calculations of Abelian[3] and non-Abelian lattice gauge theories[4] have indeed demonstrated that the strong confinement phase of lattice gauge theories is characterized by a large density of magnetic monopoles or monopole currents, if not a condensate of magnetic monopoles and antimonopoles. Also, the phase transition to the Coulomb phase in the Abelian model and the transition region to the weak-coupling region in pure SU(2) lattice theory is accompanied by a rapid decrease of the density of monopoles or monopole currents.

In this paper, we want to study the connection of topological excitations, mainly magnetic-monopole currents and vortex currents, with the different phases in the Abelian Higgs model. We use the duality transformation to obtain a suitable definition of these topological excitations and the Monte Carlo calculation to study the phase structure of the model and the properties of the three phases.

The pure Abelian U(1) lattice gauge theory is well known from Monte Carlo calculations of Lautrup and Nauenberg,[5] DeGrand and Toussaint,[6] and Bhanot.[7] The first Monte Carlo results for Abelian Higgs models were reported by Creutz[8] for $Z(2)$ and $Z(6)$ Higgs models, by Bhanot and Freedman[9] for the three-dimensional U(1) Higgs model, and by Bowler *et al.*,[10] and Callaway and Carson,[11] who studied the phase structure of the four-dimensional models with Higgs charge $q=1$ and 2 using as expectation value the average action.

Topological excitations in pure Abelian gauge models were studied using the duality transformation by Banks, Myerson, and Kogut,[12] Ukawa, Windey, and Guth,[13] Stone and Thomas,[14] and Batrouni.[15] Similar studies for the Abelian Higgs model were reported by Einhorn and Savit,[16] Peskin,[17] and Banks and Rabinovici.[18]

In Sec. II, we define the model and review its conjectured phase structure[19] as it emerges from studying the limiting models and the results of the first Monte Carlo calculations.[10,11]

In Sec. III, we write the model in terms of its topological excitations. The monopole loops and vortex sheets are found to be related to the integer parts of plaquette and link variables. We extend this analysis, which was first given for $q=1$ by Einhorn and Savit[16] to the model with Higgs charge $q\geq 1$.

In Sec. IV, we present our Monte Carlo calculation. We study first the phase structure using average plaquette and average link expectation values for the models with $q=1$, 2, and 6. Using the results of Sec. III, we give prescriptions to calculate the expectation values for monopole current densities, vortex densities, and electric current densities on the lattice. The Monte Carlo results for these quantities are given in the form of contours of equal density.

In Sec. V, we summarize the results. We find that the three phases of the model can well be characterized by the density of the topological excitations. In an appendix the phase structure of the Abelian Higgs model in four dimensions is given as it emerges from a mean-field calculation.

II. THE LATTICE ABELIAN HIGGS MODEL

We define the model in a four-dimensional hypercubical lattice. The scalar Higgs field is represented by site variables

$$S(j)=e^{i\chi(j)} . \tag{2.1}$$

The gauge field is represented by link variables

$$U_\mu(j)=e^{i\theta_\mu(j)} . \tag{2.2}$$

Both the site and link variables are elements of the U(1) group. The local gauge-invariant lattice Lagrangian is

$$\mathscr{L}=h\sum_{j,\mu}\{1-\mathrm{Re}[S(j)U_r^{\dagger q}(j)S^\dagger(j+\mu)]\}+\beta\sum_{j\mu\nu}\{1-\mathrm{Re}[U_\mu(j)U_\nu(j+\mu)U_\mu^\dagger(j+\nu)U_\nu^\dagger(j)]\} . \tag{2.3}$$

The first sum is over all links and the second sum is over all plaquettes of the lattice.

The partition function becomes, in the Wilson form of the model,

$$Z=\int_{-\pi}^{\pi}D\theta_\mu(j)D\chi(j)\exp\left[-h\sum_e\{1-\cos[\Delta_\mu\chi(j)-q\theta_\mu(j)]\}\right]\exp\left[-\beta\sum_P(1-\cos\theta_P)\right] \tag{2.4}$$

with

$$\Delta_\mu\chi(j)=\chi(j)-\chi(j+\mu) \tag{2.5}$$

and

$$\theta_P=\Delta_\mu\theta_\nu(j)-\Delta_\nu\theta_\mu(j) . \tag{2.6}$$

The charge q of the Higgs scalars is an integer multiple of the elementary charge.

The naive continuum limit of the model is obtained by the replacements

$$\begin{aligned}&\chi(j)\to\chi(\vec{x}),\ \ \theta_\mu(j)\to aA_\mu(\vec{x}),\\&\Delta_\mu\to a\nabla_\mu,\ \ \sum\to a^{-4}\int d^4x,\end{aligned} \tag{2.7}$$

and by the expansions of the cosines up to second order,

$$\mathscr{L}_{\mathrm{cont}}=\int d^4x\left[h(\nabla_\mu\chi-qA_\mu)^2+\frac{\beta}{4}F_{\mu\nu}{}^2\right] . \tag{2.8}$$

This lattice model corresponds to the conventional continuum model

$$\mathscr{L}=\tfrac{1}{2}(D_\mu\phi)^\dagger D^\mu\phi+V(\phi^\dagger\phi)+\tfrac{1}{4}F_{\mu\nu}{}^2 . \tag{2.9}$$

Replacing here

$$\begin{aligned}&V(x)=\frac{\lambda}{4!}(x-R^2)^2,\\&\phi=\rho e^{i\chi} ,\end{aligned} \tag{2.10}$$

we obtain

$$\begin{aligned}\mathscr{L}=&\tfrac{1}{2}\rho^2(\partial_\mu\chi-qeA_\mu)^2+\tfrac{1}{2}(\partial_\mu\rho)^2\\&+V(\rho^2)+\tfrac{1}{4}F_{\mu\nu}{}^2 .\end{aligned} \tag{2.11}$$

As we see, the limit model (2.8) corresponds to this model with frozen-in radial degrees of freedom of the Higgs field $(\partial_\mu\rho)^2=0$. The coupling constants of the lattice model correspond then to

$$\begin{aligned}&h\to R^2=\langle\rho^2\rangle,\\&\beta\to\frac{1}{e^2} ,\end{aligned} \tag{2.12}$$

and the gauge potentials are related,

$$A_\mu\to\frac{1}{e}A_\mu .$$

The phase structure of the lattice Abelian Higgs model in the plane of the two coupling constants β and h can be conjectured considering some limiting models.[19]

(i) For $h=0$ the model becomes the pure U(1) lattice gauge theory, which is known in four dimensions to possess a second-order phase transition near $\beta=1$ separating a confinement phase at large coupling (small β) with area behavior of the Wilson loop and the Coulomb phase at small coupling.[5–7]

(ii) For $\beta=0$ the model becomes trivial without phase transitions. In the unitary gauge, with all $\chi(j)=0$, all link variables decouple and we obtain

$$Z=\int_{-\pi}^{\pi}D\theta_\mu(j)\times\exp\left[-h\sum\{1-\cos[q\theta_\mu(j)]\}\right] . \tag{2.13}$$

This theory is exactly soluble and we get for $q=1$ for the average link,

$$\langle L\rangle=\frac{\partial}{\partial h}\frac{1}{N}\ln Z=1-\frac{I_1(h)}{I_0(h)} , \tag{2.14}$$

where I_1 and I_0 are modified Bessel functions and N is the number of links. Similarly, for the average plaquette

$$\langle P\rangle=-\frac{1}{N}\frac{\partial}{\partial\beta}\ln Z=1-(1-\langle L\rangle)^4\delta_{q,1}\;. \tag{2.15}$$

(iii) For $\beta\to\infty$, all plaquette elements become the identity. The gauge fields are gauge equivalent to total ordering and the model reduces to the XY-spin model with one phase transition at $h=0.453$.

(iv) For $h\to\infty$, the link elements become unity. In the unitary gauge this is equivalent to

$$\theta_\mu(j)=\frac{2\pi m}{q},\quad m=0,1,\ldots,q\;. \tag{2.16}$$

For $q=1$, the gauge fields are completely ordered and both $\langle L\rangle$ and $\langle P\rangle$ vanish. For $q\neq 1$, the $\theta_\mu(j)$ become Z_q variables and the model becomes the Z_q lattice gauge theory. These models[20] exhibit for $q\leq 4$ a single first-order phase transition. For $q\geq 5$, two transitions of higher order are found. With increasing q one of these transitions moves to $\beta\to\infty$ and the second survives in the $q\to\infty$ limit as the U(1) transition. For $q=2$ the critical point is at $\beta=0.4407$, for $q=6$ the two transitions occur around $\beta=1$ and $\beta=1.6$. These four limits define the boundaries of the β-h phase plane. As conjectured before,[19] these phase transitions for $q=1$ and $q=2$ were found by Monte Carlo calculations[10,11] to connect smoothly into the interior of the plane. The following picture emerges. We consider first the model for $q\geq 2$.

For small β exists a confinement phase which is connected to the corresponding phase in the limiting U(1) and Z_q models at $h=0$ and $h\to\infty$. In this phase the Wilson loop shows area behavior. For small h and larger β we find the Coulomb phase, connected to the Coulomb phase of the U(1) model at $h=0$. For $q\geq 5$ this phase is also connected to the Coulomb phase of the limiting Z_q model between the two transitions of this model. This phase is characterized by massless gauge fields and perimeter behavior of the Wilson loop.

For both β and h large we find finally the Higgs phase characterized by massive gauge fields, and perimeter behavior of the Wilson loop. In the model with $q=1$, the confinement and Higgs phase are analytically connected. In this phase external charges are screened by the Higgs fields with $q=1$. The Wilson loop shows perimeter behavior in this Higgs confinement or total screening phase.

III. MONOPOLES AND VORTICES IN ABELIAN LATTICE GAUGE THEORIES

Monopoles in Abelian theories are not of topological origin as in certain non-Abelian theories.[21] They arise due to the nonlinearities of the lattice models in the so-called electrodynamical representation of these theories.[12–17] Let us first discuss how these objects arise in the pure U(1) lattice gauge theory in four dimensions.[12,15] In this model monopoles are easily found to be independent of the lattice action used.

The partition function of the U(1) lattice theory

$$Z=\int DU_\mu(j)\exp\left[\frac{\beta}{2}\sum_{j\mu\nu}[P_{\mu\nu}(j)+P^\dagger_{\mu\nu}(j)]\right] \tag{3.1}$$

can be expressed in terms of plaquette variables

$$P_{\mu\nu}(j)=U_\mu(j)U_\nu(j+\mu)U^\dagger_\mu(j+\nu)U^\dagger_\nu(j)\;, \tag{3.2}$$

instead of the link variables $U_\mu(j)$. With this replacement (3.1) becomes[15]

$$Z=\int_{-\pi}^{\pi}\frac{D\theta_{\mu\nu}(j)}{2\pi}(j)\prod_{j\nu}\delta(e^{i\Delta_\mu\tilde\theta_{\mu\nu}(j)}-1)\times e^{\beta\sum_{j\mu\nu}\cos\theta_{\mu\nu}(j)}\;. \tag{3.3}$$

The δ functions express the lattice Bianchi identities

$$e^{i\Delta_\mu\tilde\theta_{\mu\nu}(j)}=1,\quad \tilde\theta_{\mu\nu}(j)=\tfrac{1}{2}\epsilon_{\mu\nu\rho\sigma}\theta_{\rho\sigma}(j)\;, \tag{3.4}$$

which constrain the products of plaquettes over each possible cube of the lattice. Fourier expanding the periodic δ functions,

$$\prod_{j,\nu}\delta(e^{i\Delta_\mu\tilde\theta_{\mu\nu}(j)}-1)=\sum_{m_\nu(\rho)=-\infty}^{\infty}\int_{-\infty}^{\infty}Dx_\nu\exp\left[i\sum x_\nu(\rho)[\Delta_\mu\tilde\theta_{\mu\nu}(j)+2\pi m_\nu(\rho)]\right] \tag{3.5}$$

and using the Poisson sum formula

$$\sum_{n=-\infty}^{\infty}f(n)=\sum_{n=-\infty}^{\infty}\int_{-\infty}^{+\infty}dx\,f(x)e^{2\pi i xn}\;, \tag{3.6}$$

we obtain from (3.3)

$$Z=\sum_{m_\nu(\rho)=-\infty}^{\infty}\int_{-\pi}^{\pi}D\theta_{\mu\nu}(j)\prod_{j\nu}\delta[\Delta_\mu\tilde\theta_{\mu\nu}(j)-2\pi m_\nu(\rho)]e^{\beta\sum\cos\theta_{\mu\nu}(j)}\;. \tag{3.7}$$

The lattice Bianchi identity shows the existence of the conserved monopole current $m_\nu(\rho)$,

$$\Delta_\mu \tilde{\theta}_{\mu\nu}(j)=2\pi m_\nu(\rho), \quad \Delta_\nu m_\nu(\rho)=0 . \tag{3.8}$$

$m_\nu(\rho)$ is the current on a link dual to the cube formed by $\exp[i\Delta_\mu\tilde{\theta}_{\mu\nu}(j)]$. Replacing the Wilson action by the Villain action

$$e^{\beta\cos\theta}\to e^{\beta}\sum_{l=-\infty}^{\infty}\exp\left[-\frac{\beta}{2}(\theta+2\pi l)^2\right] \tag{3.9}$$

and integrating over the plaquette variables, we find the electromagnetic representation

$$Z=\sum_{m_\nu(\rho)=-\infty}^{\infty}\left[\prod_\rho \delta(\Delta_\mu m_\mu(\rho))\right]\exp\left[-4\frac{\pi^2}{\beta}\sum m_\nu(\rho)G(\rho-\rho')m_\nu(\rho')\right] \tag{3.10}$$

with

$$\Delta_\mu\Delta_{-\mu}G(\rho-\rho')=-\delta_{\rho\rho'}, \quad \Delta_{-\mu}f(\nu)=f(\nu)-f(\nu-\mu) . \tag{3.11}$$

Next we isolate monopoles and vortices in the Abelian Higgs model,[16,17] starting from the partition function of the four-dimensional Villain model

$$Z=\sum_{a_\mu,b_{\lambda\rho}=-\infty}^{\infty}\int_{-\infty}^{\infty}D\chi\, D\theta_\mu \exp\left[-\sum_L\frac{h}{2}(\Delta_\mu\chi-q\theta_\mu+2\pi a_\mu)^2\right]\exp\left[-\sum_P\frac{\beta}{2}(\epsilon_{\rho\lambda\mu\nu}\Delta_\mu\theta_\nu+2\pi b_{\rho\lambda})^2\right] . \tag{3.12}$$

The phase structure of this model is expected to be identical to the one of the model (2.4) with the Wilson action, only the phase transitions occur at different values of the coupling parameters β and h. Therefore we might study the monopoles and vortices in the Villain version and use the Wilson action in the numerical Monte Carlo work. Fourier transforming (3.12), using

$$\exp\left[-\frac{\beta}{2}(\theta+2\pi m)^2\right]=\frac{1}{\sqrt{2\pi\beta}}\int_{-\infty}^{\infty}d\phi\exp\left[-\frac{1}{2\beta}\phi^2+i\phi(\theta+2\pi m)\right] , \tag{3.13}$$

we obtain

$$Z=\sum_{a_\mu,b_{\lambda\rho}}\int Dt_\mu Ds_{\lambda\rho}\int D\chi\, D\theta_\mu \exp\left[\sum\left[-\frac{{t_\mu}^2}{2h}+it_\mu(\Delta_\mu\chi-q\theta_\mu+2\pi a_\mu)\right]\right]$$
$$\times\exp\left[\sum\left[-\frac{{s_{\lambda\rho}}^2}{2\beta}+is_{\lambda\rho}(\epsilon_{\lambda\rho\mu\nu}\Delta_\mu\theta_\nu+2\pi b_{\lambda\rho})\right]\right] . \tag{3.14}$$

Integrating over χ and θ_μ gives the constraints

$$\prod_J \delta(\Delta_\mu t_\mu)\delta(qt_\nu+\epsilon_{\mu\nu\lambda\rho}\Delta_\mu s_{\lambda\rho}) . \tag{3.15}$$

The first constraint can be solved by setting

$$t_\nu=\epsilon_{\nu\mu\lambda\rho}\Delta_\mu A_{\lambda\rho} \tag{3.16}$$

and the second one by

$$qA_{\lambda\rho}-s_{\lambda\rho}=\tfrac{1}{2}(\Delta_\lambda s_\rho-\Delta_\rho s_\lambda) . \tag{3.17}$$

Inserting into (3.14) we obtain

$$Z=\sum_{a_\mu,b_{\lambda\rho}}\int DA_{\lambda\rho}DS_\rho \exp\left[\sum\left[-\frac{1}{2h}(\epsilon_{\mu\nu\lambda\rho}\Delta_\nu A_{\nu\rho})^2\right]\right]\exp\left[\sum(-\frac{1}{2\beta}[\tfrac{1}{2}(\Delta_\lambda S_\rho-\Delta_\rho S_\lambda)-qA_{\lambda\rho}]^2\right]$$
$$\times\exp\left[\sum 2\pi i[a_\mu\epsilon_{\mu\nu\lambda\rho}\Delta_\nu A_{\lambda\rho}+b_{\lambda\rho}(qA_{\lambda\rho}-\Delta_\lambda S_\rho)]\right] . \tag{3.18}$$

By partial summation the last exponential can be transformed into

$$\exp\left[2\pi i \sum (J_{\lambda\rho}A_{\lambda\rho}+Q_\rho S_\rho)\right] \tag{3.19}$$

with

$$J_{\lambda\rho}=q b_{\lambda\rho}+\epsilon_{\lambda\rho\mu\nu}\Delta_\mu a_\nu \tag{3.20}$$

and

$$Q_\rho=\Delta_\lambda b_{\lambda\rho},\quad Q_\rho=\frac{1}{q}\Delta_\lambda J_{\lambda\rho}\ . \tag{3.21}$$

How do we interpret these topological excitations on the dual lattice? The objects $J_{\lambda\rho}$ are associated with the plaquette λ, ρ of the dual lattice, which is dual to one plaquette of the original lattice and the Q_ρ

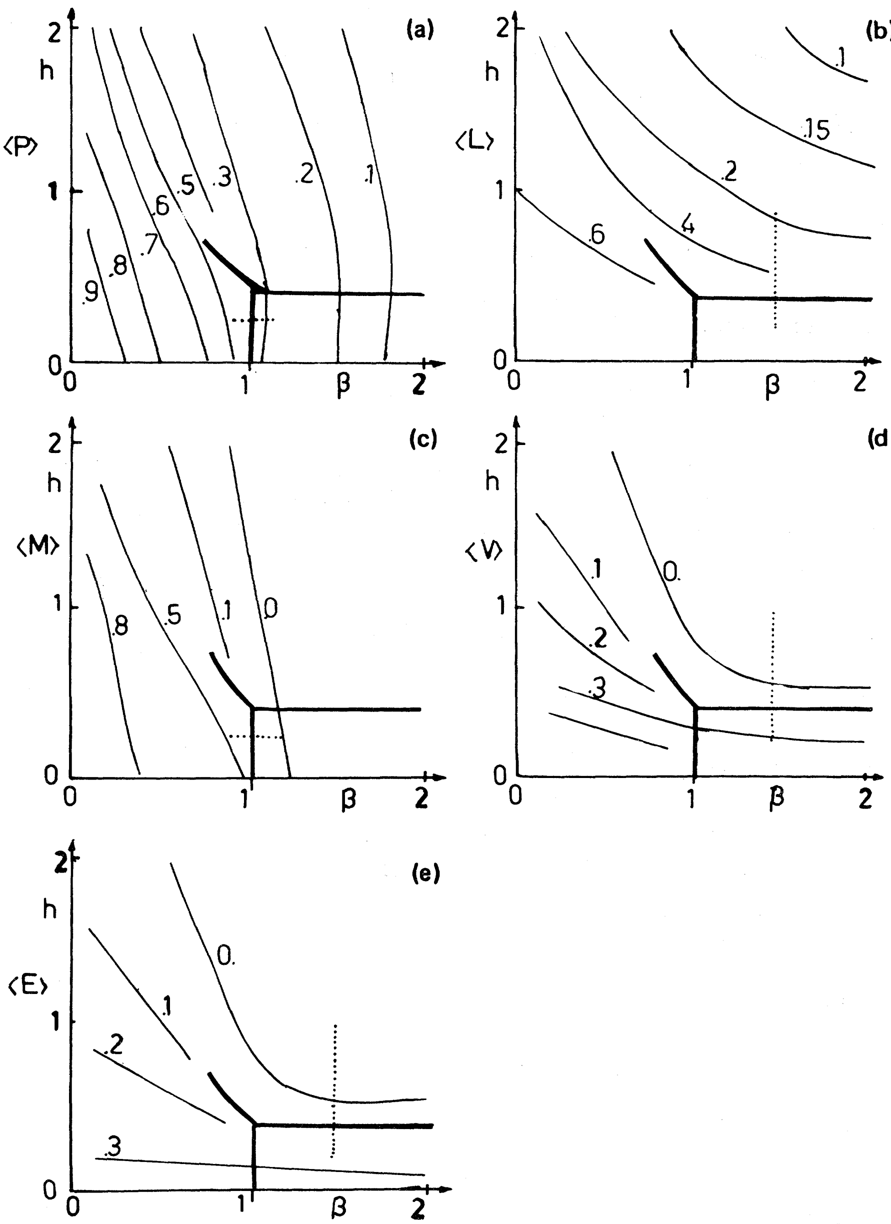

FIG. 1. Abelian Higgs model with Higgs charge $q=1$. Results of the Monte Carlo calculation on a 4^4 lattice. Given in the plane of the two coupling constants β and h are phase transition lines (thick solid lines), contours of equal values of gauge-invariant expectation values (thin solid curves), and regions of hysteresis in the expectation value considered (pointed lines). (a) Average plaquette $\langle P\rangle$, (b) average link $\langle L\rangle$, (c) average monopole current density $\langle M\rangle$, (d) average vortex current density $\langle V\rangle$, and (e) average electric current density $\langle E\rangle$. The contour lines plotted result from our Monte Carlo calculations and are therefore subject to statistical and systematic errors. The size of these errors can be estimated most easily from the original results of the sweeps through the lattice (see Fig. 4). For most of the contour plots we estimate the errors for the contours to be around ± 0.03.

live on links ρ of the dual lattice; these links are dual to one cube of the original lattice. The vortex current $J_{\lambda\rho}$ is connected to the integer part of the plaquette angle $b_{\lambda\rho}$ and the curl of the integer parts of the link angles $\Delta_\mu \chi - q\theta_\mu$. The monopole current Q_ρ is associated with the integer parts of the six plaquettes forming the cube dual to ρ on the original lattice. This interpretation of Q_ρ becomes obvious if we compare with Eq. (3.8) for the pure gauge theory. These monopole currents exist on closed loops of the dual lattice. On the XY model the vortex current $J_{\lambda\rho}$ is conserved $\Delta_\rho J_{\rho\lambda}=0$ and exists therefore only on closed surfaces of the dual lattice. In the Abelian Higgs model considered here there exist also open vortex sheets bounded by the monopole loops.

If we consider one dimension as time, the topological excitations represent the following events: The creation of a monopole-antimonopole pair connected by a vortex string and their subsequent annihilation sweeps out one of the open surfaces. The vortex strings have also dynamical degrees of freedom. Therefore we have other events, where closed loops of strings are created and subsequently annihilated. Such events sweep out closed surfaces.

In our Monte Carlo calculation to be described in the next section we use the definitions (3.20) and (3.21) as prescriptions of how to extract the vortex sheet densities and monopole loop densities from the integer parts of plaquette variables $b_{\lambda\rho}$ and link variables a_ρ. Instead of describing the topological excitations of the model entirely in magnetic terms (open and closed vortex sheets) it is sometimes more convenient to use more symmetric variables, i.e., magnetic and electric current loops. Knowing how to express the magnetic (monopole) loops in terms of the topological current density $J_{\rho\sigma}$ [compare Eq. (3.21)], one easily finds the corresponding expression for the electric loops simply by replacing $J_{\rho\sigma}$ by its dual form

$$Q^E_\sigma = \tfrac{1}{2}\epsilon_{\sigma\rho\alpha\beta}\Delta_\rho J_{\alpha\beta} \ . \tag{3.22}$$

IV. PROPERTIES OF THE LATTICE ABELIAN HIGGS MODEL AS DETERMINED BY MONTE CARLO CALCULATIONS

A. The Monte Carlo calculation

In our Monte Carlo calculation we use the Wilson action (2.4) in the unitary gauge with all $\chi(j)=0$. Furthermore, we replace the U(1) variables by Z_n variables, with $n \geq 50$,

$$U_\mu(j)=e^{i\theta_\mu(j)} \rightarrow e^{[2\pi i l_\mu(j)]/n} \ , \quad l_\mu(j)=0,1,\ldots,n-1 \ . \tag{4.1}$$

Z_n lattice gauge theories with $n\geq 5$ are known[20] to have three phases; the confinement phase and the Coulomb phase at small and intermediate values of the coupling β are equivalent to these phases of the U(1) model. The Z_n models behave differently only beyond the high β critical point around $\beta_c \approx n^2$, which is well beyond the region studied here. We generate Monte Carlo configurations of the lattice using a modified Metropolis method.[22] Depending on the computer, we use also the method of multispin-coding[20] in order to speed up the calculation and to save memory space. For most of our studies we use a 4^4 hypercubical lattice with skew periodic boundary conditions.[3] Successive configurations of the lattice are highly correlated. In order to minimize these correlations, we measure expectation values usually only after five sweeps through the entire lattice.

B. The phase diagrams

The two most elementary gauge-invariant order parameters which can be calculated for the model (2.4) are the average plaquette $\langle P\rangle$ and the average link $\langle L\rangle$,

$$\langle P(\beta,h)\rangle = -\frac{\partial}{\partial\beta}\left[\frac{1}{N_P}\ln Z(\beta,h)\right], \tag{4.2}$$

$$\langle L(\beta,h)\rangle = -\frac{\partial}{\partial h}\left[\frac{1}{N_L}\ln Z(\beta,h)\right], \tag{4.3}$$

when N_P and N_L are the total number of plaquettes and links of the lattice. We calculate these order parameters for the models with $q=1$, 2, and 6. The phase diagram for the models with $q=1,2$ is already known from Refs. 10 and 11, where however only the average action $\langle S\rangle$ is measured; therefore we restrict our study to a minimum of sweeps through the lattice necessary to measure the characteristic differences between the phases. No model with $q\geq 5$ was studied by Monte Carlo calculations before; therefore we study the model with $q=6$ in more detail in order to obtain the phase diagram.

In Figs. 1—3, we give our results for the phase diagrams of the three models with $q=1$, 2, and 6 together with contours of equal $\langle P\rangle$ and $\langle L\rangle$. For $q=1$ and 2 our results are consistent with Refs. 10 and 11. In Fig. 4 the results for one sweep through the model with $q=6$ is given for constant $h=3$ and β between 0.1 and 2.6. The phase transitions are clearly visible for the hysteresis loops obtained from sweeps with increasing and decreasing β. The average link $\langle L\rangle$ and average plaquette $\langle P\rangle$ in the model with $q=1$ behave at $\beta\rightarrow 0$ as expected from the limiting model [see Eqs. (2.14) and (2.15)].

In the Appendix, we study the phase diagram of

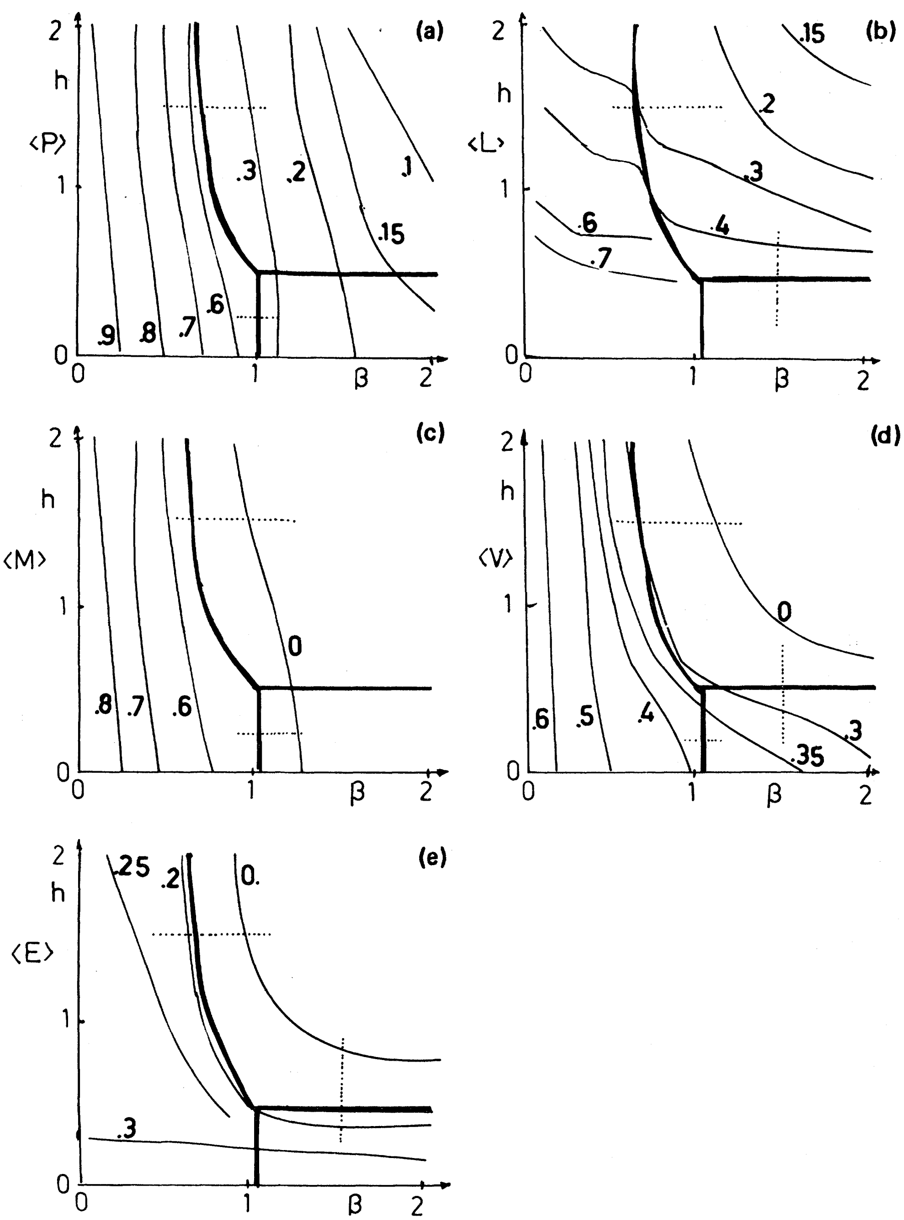

FIG. 2. Abelian Higgs model with Higgs charge $q=2$. For further explanations see caption of Fig. 1.

the three models using the mean-field method. The phase diagrams obtained by the mean-field method are consistent with the Monte Carlo result with two important exceptions.

(i) In the model with $q=1$, the mean-field theory does not find that the phase transition between confinement and the Higgs phase terminates as found in the Monte Carlo calculations and as demanded by the Osterwalder-Seiler analyticity.[23]

(ii) In the model with $q=6$, the mean-field theory does not find the two phase transitions in the limiting Z_6 model at $h\rightarrow\infty$; therefore the Higgs transition between the Higgs and Coulomb phases and the confinement transition between the confinement and the Coulomb phases meet in the center of the plane of both coupling parameters. In the model with $q=6$ we find two well-separated phase-transition lines.

(1) The confinement transition between the confinement and Coulomb phase. The critical line is a straight line at $\beta\approx 1$ from the critical point of the U(1) model at $h=0$ to the first critical point in the Z_6 model at $h\rightarrow\infty$.

(2) The Higgs transition between the Coulomb and Higgs phases. This critical line joins the second critical point of the limiting Z_6 model to the critical

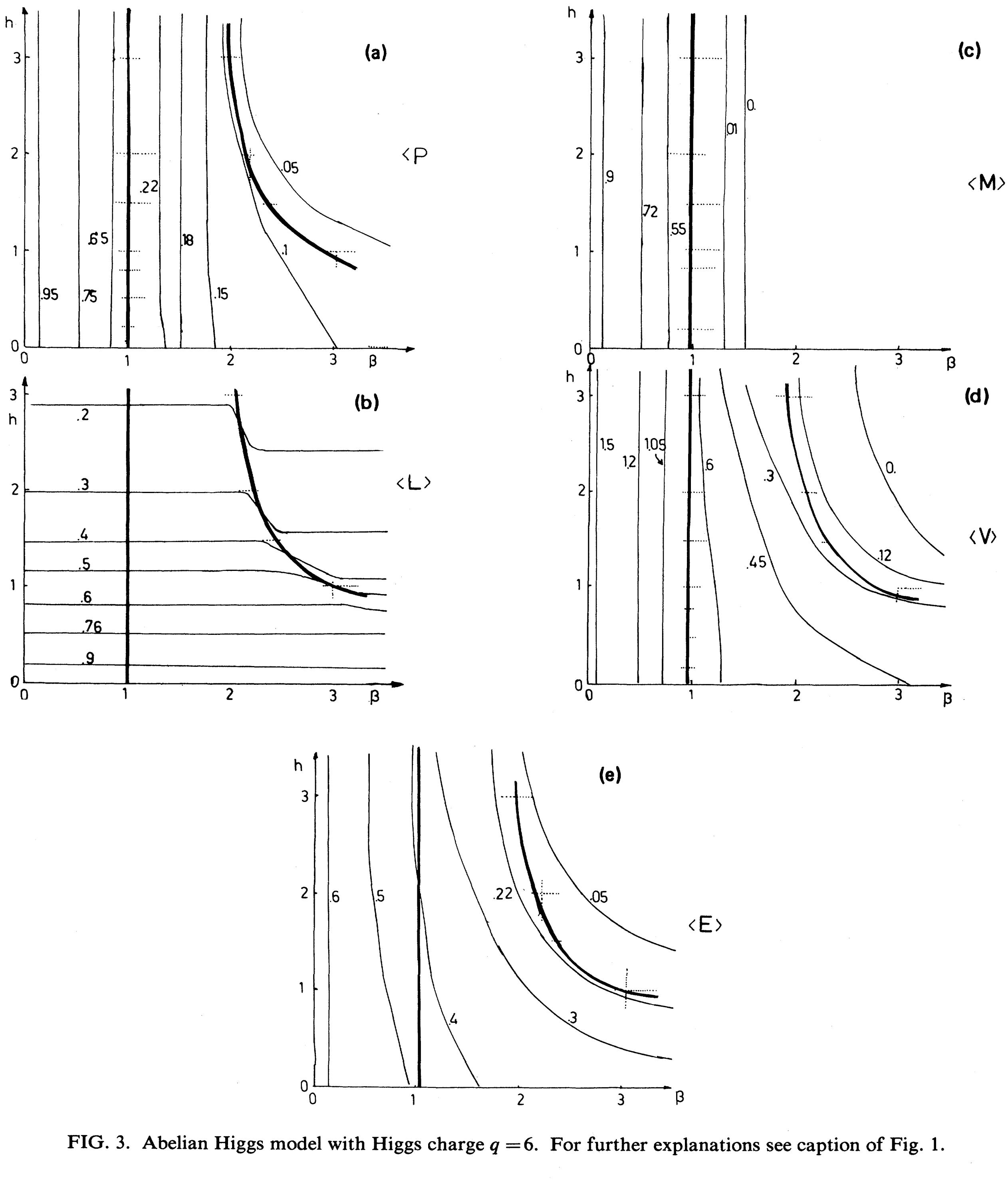

FIG. 3. Abelian Higgs model with Higgs charge $q=6$. For further explanations see caption of Fig. 1.

point of the limiting XY model at $\beta\rightarrow\infty$. We did perform mixed phase runs around the phase transition between the Coulomb and Higgs phases. This transition is very weak and we could not find in the Monte Carlo runs any evidence for a phase transition of first order.

B. Topological excitations, monopole current densities, vortex current densities, and electric current densities

The lattice definition of magnetic-monopole loops in the pure U(1) gauge theory and in the Abelian

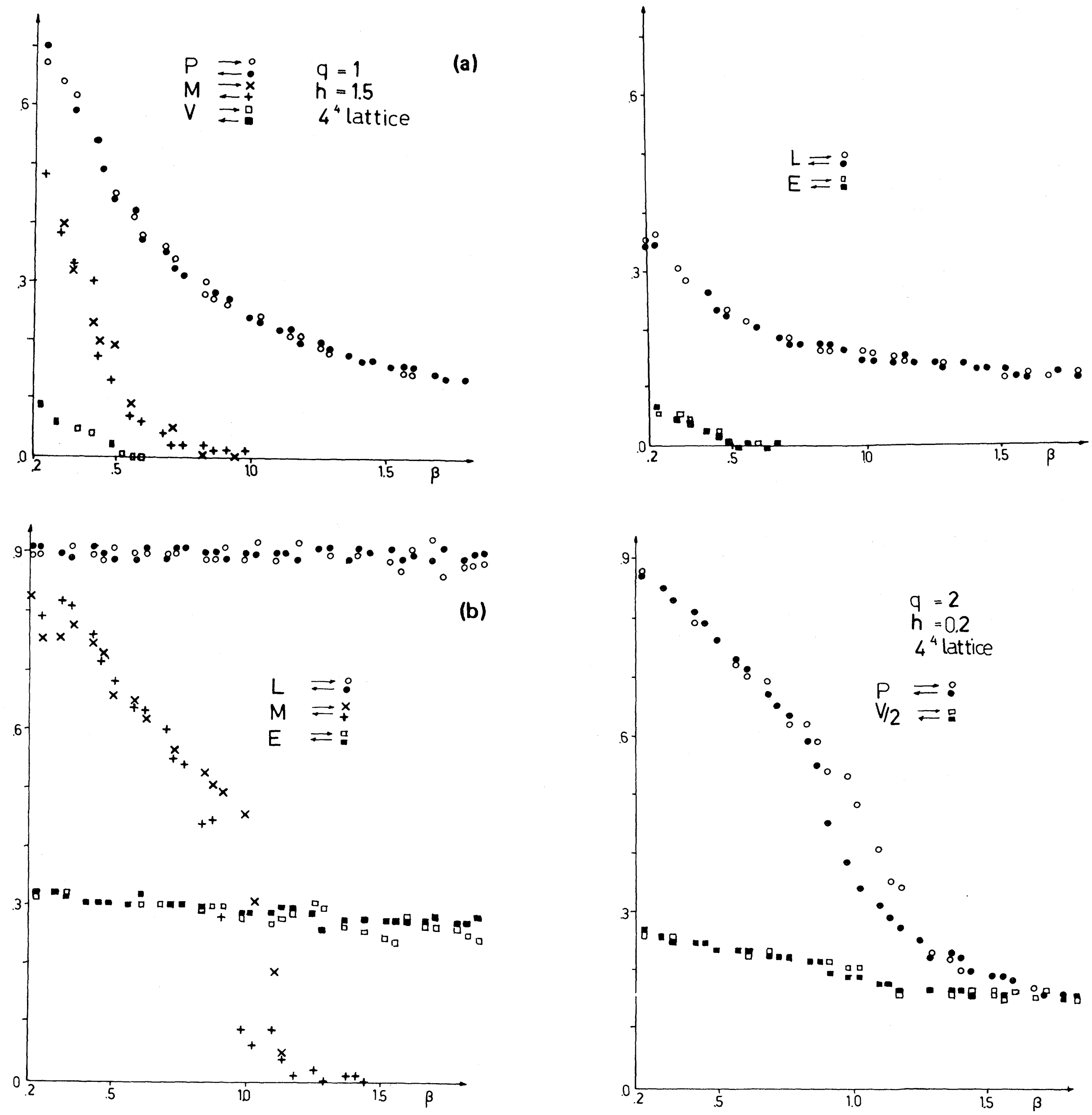

FIG. 4. Examples for the results of one single scan through the lattice as a function of the coupling constant along a line of constant coupling h. Plotted for increasing and decreasing β values are the following gauge-invariant expectation values: average plaquette $\langle P \rangle$, average link $\langle L \rangle$, average monopole current density $\langle M \rangle$, average vortex current density $\langle V \rangle$, and average electric current density $\langle E \rangle$. (a) Abelian Higgs model with Higgs charge $q=1$, (b) Abelian Higgs model with Higgs charge $q=2$, (c) Abelian Higgs model with Higgs charge $q=6$.

Higgs model follow from (3.8) and (3.21). DeGrand and Toussaint[3] were the first to study U(1) monopoles on the lattice.

We first decompose the U(1) plaquette angles

$$\vartheta_{\rho\lambda}=\tfrac{1}{2}\epsilon_{\rho\lambda\mu\nu}\Delta_\mu\theta_\nu$$

into two pieces, the fluctuating part $\widetilde{\vartheta}_{\rho\lambda}$ in the range $-\pi \le \widetilde{\vartheta}_{\rho\lambda} \le \pi$ and the integer part $2\pi b_{\rho\lambda}$,

$$\vartheta_{\rho\lambda}=\widetilde{\vartheta}_{\rho\lambda}+2\pi b_{\rho\lambda} \ . \tag{4.4}$$

Note, that ρ and λ denote directions of the dual lat-

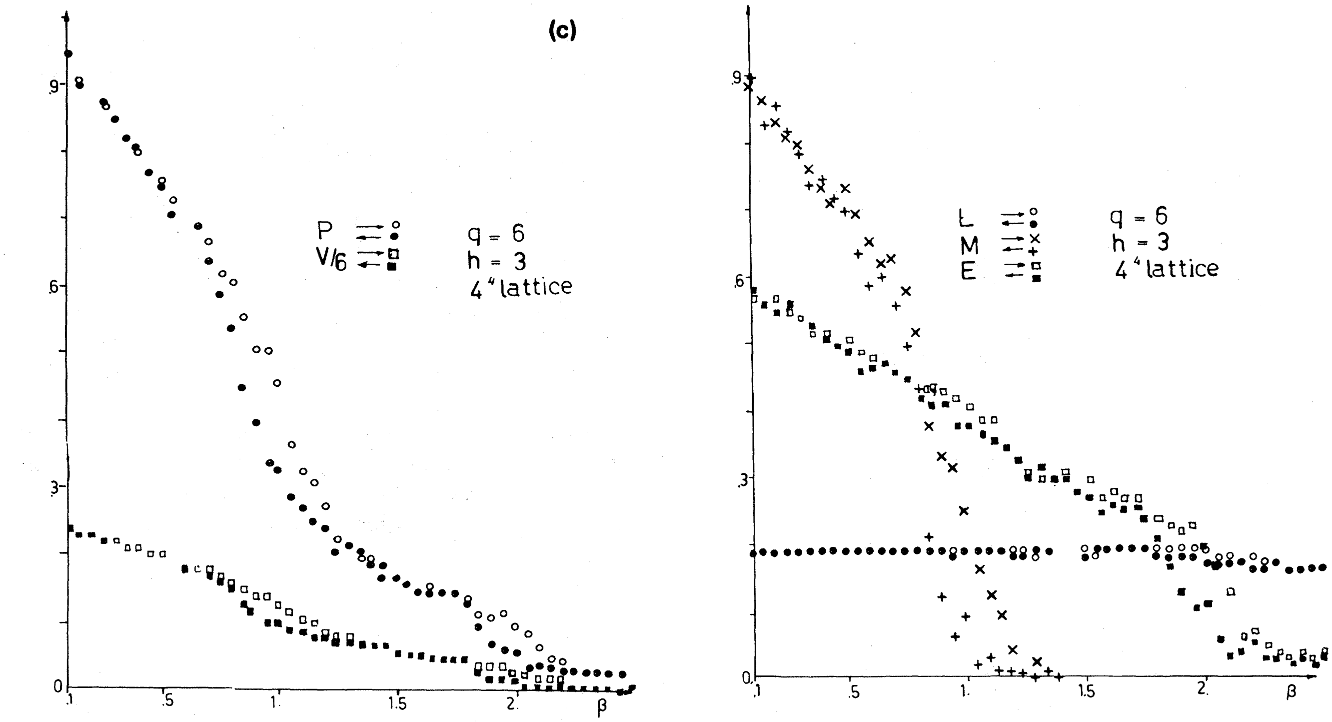

FIG. 4. (*Continued.*)

tice. The integer part represents one vortex or Dirac string carrying one unit 2π of flux. We can measure the number of monopoles inside a three-dimensional box by counting the number of strings terminating inside the box,

$$2\pi Q_\rho = \sum_{\text{surfaces}} \tilde{\vartheta}_{\rho\lambda} = 2\pi \sum_{\text{cubes}} \Delta_\lambda b_{\lambda\rho} \ . \tag{4.5}$$

In four dimensions we get the density of monopole loops $\langle M \rangle = \langle Q_\rho \rangle$ by considering the monopoles in each elementary three-dimensional cube of the lattice.

We see from (3.21), that the definition of the monopole loop density in the Abelian Higgs model is completely analogous to the pure U(1) model. To define the monopoles, we need only the integer parts $b_{\mu\nu}$ of the plaquette variables. In the Abelian Higgs model there are, according to (3.20), two pieces contributing to the vortices, or Dirac strings, through one elementary plaquette. The first part is q times the integer part of the plaquette angle, the second part is the curl of the integer parts of the link angles a_ν. In unitary gauge the link angle in our Wilson action is

$$\theta_L = -q\theta_\mu \ . \tag{4.6}$$

The link variables take values $0 \le \theta_\mu \le 2\pi$, therefore θ_L varies in the range $-2\pi q \le \theta_L \le 0$. We decompose θ_L into a fluctuating piece $\tilde{\theta}_L$ in the range $-\pi \le \tilde{\theta}_L \le \pi$ and the integer part a_μ

$$\theta_L = \tilde{\theta}_L + 2\pi a_\mu \ . \tag{4.7}$$

These are the integers a_μ which we use in the definition of the vortex sheets (3.20).

The definition of the integer parts a_μ and $b_{\rho\mu}$ of the link and plaquette variables in the Wilson theory in Eqs. (4.7) and (4.4) is by no means unique. For link variables in the range $-\pi \le \theta_\mu \le \pi$ and for $q=1$, the integer part a_μ of the link variables according to (4.7) would even disappear. For any definition of these integer parts, however, the expectation values $\langle M \rangle$, $\langle V \rangle$, and $\langle E \rangle$ which we study in Figs. 1 to 3 will exhibit a characteristic transition across the phase transition lines. Our choice (4.7) and (4.4) leads to a vanishing vortex density $\langle V \rangle$ in the Higgs phase for any value of q. Other definitions would lead to identical expectation values only in the limit $q \to \infty$.

Besides the average monopole loop density $\langle M \rangle = \langle Q_\rho \rangle$ and average vortex sheet density $\langle V \rangle = \langle J_{\lambda\rho} \rangle$, we study also the electric current density

$$Q_\sigma^E = \tfrac{1}{2} \epsilon_{\sigma\rho\alpha\beta} \Delta_\rho J_{\alpha\beta} \tag{4.8}$$

and calculate the average electric current density $\langle E \rangle = \langle Q_\sigma^E \rangle$. Q_σ^E is defined on the six plaquettes (in four dimensions) which form the coboundary of the link σ. Therefore $\langle E \rangle$ is also a measure for the density of small closed vortex sheets, while $\langle M \rangle$ indicates the presence of open vortex sheets bounded

TABLE I. Properties of phases and phase transitions of the Abelian Higgs model

	Wilson loop $\langle W \rangle$ behavior	Potential	Average plaquette $\langle P \rangle$	Average link $\langle L \rangle$	Monopole loop density $\langle M \rangle$	Vortex current density $\langle V \rangle$	Electric current density $\langle E \rangle$
Phases							
Confinement	Area	Linear	Large	Large	Large	Large	Large
Coulomb	Perimeter	Coulomb	Medium	Large	$\to 0$	Medium	Large
Higgs	Perimeter	Yukawa	Small	Small	0	$\to 0$	$\to 0$
Higgs confinement ($q=1$)	Perimeter	Yukawa	Decreasing	Dcreasing	Decreasing	Decreasing	Decreasing
Phase transitions							
Confinement			Decreasing	Constant	Decreasing	Decreasing	Constant
Higgs ($q=6$)			Decreasing	Decreasing	0	Decreasing	Decreasing

by monopole loops.

In Figs. 1 to 3 we present the monopole current densities $\langle M \rangle$, vortex current densities $\langle V \rangle$, and electric current densities $\langle E \rangle$ as determined in the Monte Carlo calculation for the models with $q=1$, 2, and 6. We find the following.

(i) In the confinement phases of the models with $q=2$ and $q=6$, there is a large monopole current density $\langle M \rangle$. The confinement transition is characterized by a rapidly dropping monopole current density. Beyond the phase transition in the Coulomb or Higgs phase, $\langle M \rangle$ is exponentially decreasing. The vortex density $\langle V \rangle$ and electric current density $\langle E \rangle$ are both large in the confinement phase. In the model with $q=1$, $\langle M \rangle$ is big only near the confinement phase of the limiting U(1) model at $h=0$ and decreases rapidly with decreasing h in the confinement-Higgs phase. The $\langle V \rangle$ and $\langle E \rangle$ ex-

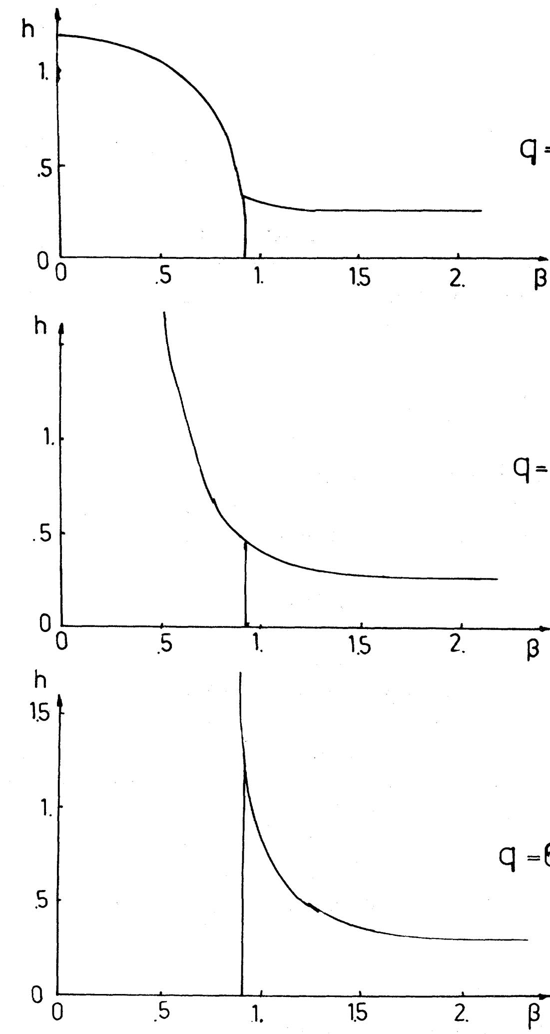

FIG. 5. Phase diagrams for the Abelian Higgs model with Higgs charges $q=1$, $q=2$, and $q=6$ computed with the mean-field method.

pectation values behave quite similarly.

(ii) Entering the Coulomb phase from the confinement phase, $\langle M \rangle$ vanishes rapidly. The vortex current density $\langle V \rangle$ drops also rapidly across the confinement transition but remains finite everywhere in the Coulomb phase. The electric current density $\langle E \rangle$ does not change significantly across the confinement transition and stays finite in the Coulomb phase.

(iii) The vortex current density $\langle V \rangle$ and electric current density $\langle E \rangle$ drop rapidly across the Higgs transition and vanish exponentially in the Higgs phase.

(iv) The vortex current density $\langle V \rangle$ gets contributions from open vortex sheets bounded by monopole loops and from closed vortex sheets. We find, indeed, that $\langle V \rangle$ behaves roughly like $\langle M \rangle + \langle E \rangle$.

V. SUMMARY

In Table I we summarize the properties of the phases and phase transitions of the Abelian Higgs model as found in our calculations. The phase structure found is consistent with expectations from limiting models[19] and for $q=1$ and 2 consistent with previous Monte Carlo studies.[10,11] The three phases of the model can be characterized by densities of topological excitations. In particular, the confinement phase is characterized by a large density of monopole currents and the Higgs phase by a vanishing density of monopole, vortex, and electric current densities. In the Coulomb phase only the vortex and electric current density remain finite. These properties become especially transparent in the model with $q=6$, where the confinement transition and the Higgs transition are well separated.

ACKNOWLEDGMENTS

We acknowledge the assistance of K. Hänssgen and S. Henger in running computer programs and helpful discussions with H.-J. Pohle.

APPENDIX: MEAN-FIELD APPROXIMATION TO THE ABELIAN HIGGS MODEL

Mean-field techniques[24] are very useful in estimating the phase diagram of various lattice models. Surprisingly accurate results have been obtained for the gauge groups $Z(2)$, U(1), SO(3), and SU(N), as well as for SU(2)−SU(3) mixed models.[25] Here we study the Abelian Higgs model in mean-field approximations.

In this approach one studies a single link or site variable assuming that fields on neighboring links and sites take average values to be determined self-consistently. We denote the average gauge field by

$$\langle U_\mu \rangle = \langle e^{i\theta_\mu} \rangle = m \tag{A1}$$

and the average Higgs field by

$$\langle S \rangle = \langle e^{i\chi} \rangle = M \ . \tag{A2}$$

From the full action (2.3) we thus find the effective single-link action

$$S_{\text{eff}}(U) = 2(d-1)\frac{\beta m^3}{2}(U+U^\dagger) + \frac{h}{2}M^2[U^q + (U^\dagger)^q] \tag{A3}$$

and similarly for the Higgs field

$$S_{\text{eff}}(S) = \frac{h}{2} 2dMm^q(S+S^\dagger) \ . \tag{A4}$$

d is the number of space-time dimensions. There are $2(d-1)$ neighboring plaquettes and $2d$ neighboring links, respectively. We are now looking for self-consistent solutions, i.e., nontrivial solutions of the coupled equations

$$M = \frac{d}{dz_3}\ln\int_0^{2\pi} d\chi \exp(z_3\cos\chi) = \frac{I_1(z_3)}{I_0(z_3)} \ , \tag{A5}$$

$$m = \frac{d}{dz_1}\ln\int_0^{2\pi} d\theta\, e^{z_1\cos\theta + z_2\cos(q\theta)} \tag{A6}$$

with

$$z_1 \equiv 2(d-1)\beta m^3, \quad z_2 \equiv hM^2, \quad z_3 \equiv 2dhMm^q \ . \tag{A7}$$

M and m appear as order parameters. The various phases are characterized in the following way:

Confinement phase:	$M=m=0$,
Coulomb phase:	$M=0, \ m\neq 0$,
Higgs phase:	$M\neq 0, \ m\neq 0$.

The transition between the Coulomb and Higgs phases is most easily analyzed. Approaching the transition from the Higgs phase, M goes to zero in a square-root-type fashion. As a function of β one finds a critical coupling h_{crit},

$$h_{\text{crit}}(\beta) = \frac{1}{4m^q} \tag{A8}$$

with m being the solution of

$$m = \frac{I_1(z_1)}{I_0(z_1)} \ . \tag{A9}$$

For large β h_{crit} approaches

$$h_{\text{crit}} \underset{\beta\to\infty}{\longrightarrow} \tfrac{1}{4} \ , \tag{A10}$$

independent of the Higgs charge q. This is to be compared with the critical coupling $h^{xy}_{\text{crit}}=0.453$ of the XY model.

In order to find the complete phase diagram, a modest amount of numerical analysis is required. Results are shown in Fig. 5. For $q=1$, a phase line separating the would-be confinement and Higgs phase extends down to the $\beta=0$ axis. It is of course well known that for $q=1$ these two regions are actually analytically connected. More refined mean-field techniques[26] should remedy this problem. For larger q values the mean-field approach still yields a triple point in the interior of the phase plane. This is in disagreement with Monte Carlo results showing two disconnected phase lines. This problem already arises for Z_q theories where the second phase transition (moving with q) is not found by mean-field methods. It is not quite clear how to resolve this problem.

[1]K. Wilson, Phys. Rev. D 10, 2445 (1974).
[2]M. Creutz, Phys. Rev. Lett. 45, 313 (1980).
[3]T. A. DeGrand and D. Toussaint, Phys. Rev. D 22, 2478 (1980).
[4]I. G. Halliday and A. Schwimmer, Phys. Lett. 102B, 337 (1981); L. Caneschi, I. G. Halliday, and A. Schwimmer, Nucl. Phys. B200, 409 (1982); R. Brower, D. Kessler, and H. Levine, Phys. Rev. Lett. 47, 621 (1981); R. Brower, D. Kessler, and H. Levine, Nucl. Phys. B205, 77 (1982).
[5]B. Lautrup and M. Nauenberg, Phys. Lett. 95B, 63 (1980).
[6]T. A. DeGrand and D. Toussaint, Phys. Rev. D 24, 466 (1981).
[7]G. Bhanot, Phys. Rev. D 24, 461 (1981); Princeton report, 1981 (unpublished).
[8]M. Creutz, Phys. Rev. D 21, 1008 (1980).
[9]G. Bhanot and B. A. Freedman, Nucl. Phys. B190, 357 (1981).
[10]K. C. Bowler, G. S. Pawley, B. J. Pendleton, D. J. Wallace, and G. W. Thomas, Phys. Lett. 104B, 481 (1981).
[11]D. J. E. Callaway and L. J. Carson, Phys. Rev. D 25, 531 (1982).
[12]T. Banks, R. Myerson, and J. Kogut, Nucl. Phys. B129, 493 (1977).
[13]A. Ukawa, P. Windey, and A. H. Guth, Phys. Rev. D 21, 1013 (1980).
[14]M. Stone and P. R. Thomas, Phys. Rev. Lett. 41, 351 (1978).
[15]G. G. Batrouni, Berkeley Report No. LBL 13424, 1981 (unpublished).
[16]M. B. Einhorn and R. Savit, Phys. Rev. D 17, 2583 (1978).
[17]M. E. Peskin, Ann. Phys. (N.Y.) 113, 122 (1978).
[18]T. Banks and E. Rabinovici, Nucl. Phys. B160, 349 (1979).
[19]E. Fradkin and S. H. Shenker, Phys. Rev. D 19, 3682 (1979).
[20]M. Creutz, L. Jacobs, and C. Rebbi, Phys. Rev. D 20, 1915 (1979).
[21]For a review, see P. Goddard and D. Olive, Rep. Prog. Phys. 41, 91 (1978).
[22]N. Metropolis, A. W. Rosenbluth, N. N. Rosenbluth, A. H. Teller, and E. Teller, J. Chem. Phys. 21, 1087 (1953); K. Binder, in *Phase Transitions and Critical Phenomena*, edited by C. Domb and M. S. Green (Academic, New York, 1976), Vol. 5B.
[23]K. Osterwalder and E. Seiler, Ann. Phys. (N.Y.) 110, 440 (1978).
[24]K. Wilson, Phys. Rev. D 10, 2445 (1974); R. Balian *et al., ibid.* 11, 2104 (1975).
[25]J. Greensite and B. Lautrup, Phys. Lett. 104B, 41 (1981); D. Pritchard, *ibid.* 106B, 193 (1981).
[26]J. M. Drouffe, Nucl. Phys. B170, 211 (1980); Phys. Lett. 105B, 45 (1981); B. Lautrup, in talk at the 13th Spring Symposium on High Energy Physics, Bad Schandau (unpublished).